CUTTLEFISH BONE-BASED INK FOR 3D PRINTING OF SCAFFOLDS FOR ORTHOPEDIC APPLICATIONS

Filis CURTI[1], Diana-Maria DRĂGUȘIN[2], Andrada SERAFIM[3], Anca SORESCU[4], Izabela-Cristina STANCU[5], Horia IOVU[6], Rodica MARINESCU[7]

Marine origin materials, such as cuttlefish bone, have attracted significantly interest due to their outstanding features. Cuttlefish bone is a promising alternative as biogenous bone for bone tissue healing, considering its composition based primarily on calcium carbonate, its biocompatibility, osteoconductivity and bioactivity. In this work, a novel organic/inorganic paste-type ink containing cuttlefish bone was developed for the fabrication of 3D printed scaffolds as promising structures for bone defects. The biogenous bone acts as a reinforcing filler, improving significantly the mechanical properties of gelatin/alginate hydrogel.

Keywords: cuttlefish bone, reinforcing filler, 3D printing, paste-type ink

1. Introduction

Marine origin materials have been extensively studied as promising materials for hard tissue replacement due to their extraordinary mechanical, chemical and physical properties [1], [2]. Cuttlefish bone (CB) is a promising nature-created material which possesses appealing properties for biomedical, pharmacological and non-pharmacological (calcium supplements) applications [3]. It is an ultra-lightweight worldwide available material with low cost, high permeability and unique porous structure, due to its two structural segments (dorsal shield and lamellar matrix, respectively) [1], [3]–[9]. The dense dorsal shield acts as a rigid

[1] PhD student, Advanced Polymer Materials Group, University POLITEHNICA of Bucharest, Romania, e-mail: c.filis7@yahoo.com
[2] Lecturer, Advanced Polymer Materials Group, University POLITEHNICA of Bucharest, Romania, e-mail: diana.m.dragusin@gmail.com
[3] PhD, researcher, Advanced Polymer Materials Group, University POLITEHNICA of Bucharest, Romania, e-mail: andrada.serafim@gmail.com
[4] Master Student, Smart Biomaterials and Applications, Faculty of Medical Engineering, University POLITEHNICA of Bucharest, Romania, e-mail: sorescu.anca@gmail.com
[5] Professor, Advanced Polymer Materials Group, University POLITEHNICA of Bucharest, Romania, e-mail: izabela.stancu@upb.ro
[6] Professor, Advanced Polymer Materials Group, University POLITEHNICA of Bucharest, Romania, e-mail: horia.iovu@upb.ro
[7] Associate Professor, Department of Orthopedy, Colentina Clinical Hospital, Bucharest, Romania, e-mail: rodicamarinescu@ymail.com

protecting substrate to facilitate the development of the porous internal lamellar matrix which acts as a floating tank and withstand at high hydrostatic pressure [1], [4], [9]. The lamellar matrix is primarily composed of calcium carbonate (aragonite phase) associated with organic components (mainly β-chitin) [1], [4], [6], [8], [10], [11].

In Chinese traditional medicine, CB was used for its hemostatic properties or for the treatment of gastritis [3], [11]. Nowadays, it is used to produce calcium phosphate materials via a hydrothermal reaction [1], [2], [4], [12], [13], or used as an attractive reinforcing filler [5], [8], [14]–[16]. The outstanding biocompatibility, bioactivity and osteoconductivity features sustain CB potential for bone regeneration [7], [11], [17], [18]. It was already investigated as potential xenogeneic graft, and it promoted the bone healing [17], [18].

A previous study reported by our group highlighted the potential of CB powder as reinforcing agent for gelatin/alginate hydrogel precursor, in comparison with other well-known minerals [5]. Based on the outstanding results in terms of mechanical and biological properties reported for the hybrid hydrogel loaded with CB [5], the development of 3D printed scaffolds with well-defined architecture was considered in this work, by formulating a printable ink containing this biogenous material. 3D printing is an additive manufacturing technique based on layer-by-layer deposition, which produces advanced 3D scaffolds that match the predesigned model closely. Both gelatin and sodium alginate (SA) are well-known biopolymers to formulate printable inks, and their combination was widely used for 3D printing [19]. Although mammalian gelatins are the most extensively used in ink preparations, the fish gelatin (FG) is a promising marine-derived candidate that allows the preparation of high concentrated aqueous solutions and avoids the risk of bovine spongiform encephalopathy disease transmission [20], [21].

The present work proposed the formulation of a thick-paste type ink based on exclusively marine resources such as FG, SA and CB to fabricate high-performant 3D printed scaffolds. Such concentrated combination has major claims to a novel approach since, to the best of authors' knowledge, this was not previously reported in the literature. The high concentration of FG solution and the substantial incorporation of SA and CB powders were chosen in an attempt to fabricate 3D printed composite scaffolds with outstanding mechanical features and potential applicability in bone tissue engineering. A crosslinking study was conducted, and the gel fraction was determined to appreciate the crosslinking efficiency. Swelling ability, dimensional stability and degradation behavior were investigated, and, for the mechanical properties, the Young modulus was determined. Micro-computed tomography (Micro-CT) was used for the morpho-structural characterization of the 3D scaffolds.

2.Materials and methods

2.1. Materials

FG (gelatin from cold water fish skin) and SA (medium viscosity alginic acid sodium salt from brown algae), glutaraldehyde (50% aqueous solution, GA), calcium chloride and phosphate buffered saline (PBS, 0.01 M, pH 7.4, prepared as indicated by the manufacturer) were supplied by Sigma-Aldrich. CB was purchased from pet stores (Romania). A GFL distiller apparatus was used for double distilled water (ddw).

2.2. Methods

2.2.1. Preparation of CB powder

The dorsal shield of CB was removed, and the lamellar part was cut into smaller blocks which were extensively washed with ddw, and then dried. Further, the CB blocks were crushed, and a milled powder was obtained. The finely fraction was collected by powder separation through several decanting steps in ddw, and subsequently dried.

2.2.2. Ink formulation

A 50 wt.% FG aqueous solution was prepared under stirring at 40°C. The three components FG:CB:SA were mixed in a mass ratio of 43:34:23, as described below. The necessary amounts of SA and CB powders were mixed, and subsequently, the powder mixture was mechanically incorporated within the FG solution to obtain the paste-type ink. A possible crosslinking of polysaccharide phase may start from this preparation stage due to the carbonate content of CB.

2.2.3. 3D printing manufacturing

Fish gelatin/cuttlebone/alginate (FGCA) scaffolds were fabricated using the Direct Dispenser DD135N printhead of the 3D Discovery Bioprinter (RegenHU, Switzerland). The 3D object was design in BioCAD software (developed by RegenHU, Switzerland) as a rectangular block with 10 x 10 mm^2 base, 6 layers of 0^o-90^o deposition direction, and a 1 mm distance between two neighboring filaments. An ".iso" file containing the established parameters was generated and loaded in 3D Discovery HMI software (RegenHU, Switzerland).

The ink was loaded into a 3 mL syringe, and a conical nozzle of 0.25 mm inner diameter (G25) was attached to the syringe. Multiple trials were performed to determine the most suitable printing parameters. For an adequate extrusion, the ink was pressurized at 550 ± 30 kPa with a feed rate of 1 mm/s. The 3D scaffolds were printed on a plastic sheet at room temperature.

2.2.4. Post-printing stabilization through crosslinking

The 3D printed scaffolds were kept in the refrigerator before crosslinking to facilitate the physical gelation of the protein component. A two-step crosslinking

method was proposed. The 3D structures were initially exposed to vapors of GA up to 48 hours. The second step involved the samples immersion in a crosslinking bath. A crosslinking study was performed to choose the right composition of crosslinking media based on calcium chloride and GA for the combined crosslinking of SA and FG. 1% GA was used, while calcium chloride concentration was varied, thus 3C1G containing 3%, 4C1G containing 4% and 5C1G containing 5% calcium chloride. For each crosslinking bath, four specimens were used, and the immersion period was 4 days. The gel fraction (GF) analysis was performed to appreciate the crosslinking efficiency of each tested bath. After crosslinking step, all samples (except the specimens for GF) were extensively washed for 2 days considering the extraction and removal of non-reacted crosslinking agents, followed by drying to constant mass.

2.2.5. Characterization of hybrid printed scaffolds

GF analysis. The crosslinking efficiency was assessed by gravimetrically determination of GF. The dried crosslinked samples were incubated in ddw at 37ºC for 48 hours to facilitate the soluble fraction extraction. GF was computed using equation (1):

$$GF, \% = \frac{w_{\alpha 1}}{w_{\alpha 0}} \, x \, 100 \quad (1)$$

where $w_{\alpha 0}$ is the initial weight of dried crosslinked scaffolds before extraction in ddw and $w_{\alpha 1}$ is the weight of the dried samples after extraction.

Micro-CT. A SkyScan 1272 high-resolution X-Ray microtomograph (Bruker MicroCT, Belgium) was used to visualize the 3D printed samples and investigate the CB distribution. The dried sample was fixed on the scanning stage using dental wax. The scanning was performed at a 2452 x 1640 resolution and a 1.75 µm pixel size, using a voltage of 60 kV and an intensity of 150 µA. The images were registered with a rotation step of 0.3º and an averaging of 3 frames, at an exposure time of 700 ms. The resulted cross-sections were processed using CT NRecon software and subsequently reconstructed using CTVox.

Swelling behavior evaluation. The swelling ability of the crosslinked FGCA scaffolds was checked by immersion in PBS up to 30 hours, at 37ºC. The test was performed in triplicate and the swelling degree (SD, %) was determined gravimetrically using equation (2):

$$SD, \% = \frac{w_{tf} - w_{ti}}{w_{ti}} \, x \, 100 \quad (2)$$

where w_{ti} represents the initial weight of dried scaffold prior to PBS incubation and w_{tf} denotes the weight of swollen FGCA specimens at the pre-established immersion time, t. The equilibrium PBS content (EC_{PBS}, %) was computed when the equilibrium point was reached at corresponding w_{tf}, and was determined using the equation (3):

$$EC_{PBS}, \% = \frac{w_{tf} - w_{ti}}{w_{tf}} \; x \; 100 \quad (3)$$

Dimensional stability. The changes for length (L), width (W) and height (H) of the 3D printed scaffolds were determined to assess the dimensional stability in aqueous fluids. The L, W and H dimensions of the scaffolds were measured in both conditions, dried and rehydrated, respectively, using a digital caliper. A graphical representation was plotted based on the dimensional variations (Δd, %). These variations in terms of L, W and H were computed using the equation (4):

$$\Delta d, \% = \frac{d_h - d_d}{d_d} \; x \; 100 \quad (4)$$

where d_d is the L / W / H of the samples in dried state and d_h is the L / W / H of the samples in rehydrated state. The test was performed in triplicate.

Stability test in PBS. The stability behavior of 3D printed FGCA scaffolds was assessed in 0.01M PBS (pH 7.4) at 37°C. The test was performed in triplicate, and the specimens were kept in individual test tubes containing 20mL of PBS, for 7 and 28 days. The degradation degree (DD, %) was computed using equation (5):

$$DD, \% = \frac{w_{bd} - w_{ad}}{w_{bd}} x100 \quad (5)$$

where w_{bd} is the weight of dried FGCA samples before testing and w_{ad} is the weight of dried PBS-treated samples.

Fourier transform infrared (FTIR)analysis. A JASCO 4200 spectrometer equipped with a Specac Golden Gate attenuated total reflectance (ATR) device was used to investigate the spectral changes caused by degradation experiment. The spectra of the raw materials (FG, CB, SA) and FGCA samples, before and after incubation in PBS, were recorded in the 4000 – 600 cm^{-1} wavenumber regions, at a resolution of 4 cm^{-1}.

Mechanical properties evaluation. A Brookfield CT3 texture analyzer with a 4500 grams cell load (Brookfield Engineering) in compression mode was used. The scaffolds were rehydrated in PBS to reach the swelling equilibrium. The test was performed in triplicate and the scaffolds dimensions were measured using a digital caliper. The rehydrated specimens were placed on a plate and uniaxial pressed by the mechanical cell, at the compression speed of 0.1 mm/s. Stress-deformation curves were plotted and the values of Young modulus of FGCA scaffolds (before and after degradation) were established based on the slope of the initial linear part of compression curve, at a strain of 1%.

3. Results and discussion

In this study, a concentrated ink based on FG, SA and CB was formulated for the development of 3D printed scaffolds with appealing properties for bone defects. The incorporation of mineral phase-containing CB into the gelatin/alginate hydrogel is a biomimetic approach considering the structural and compositional characteristics of bone tissue. The potential of the FGCA printed scaffold was investigated in terms of stability and mechanical properties for biomedical applications.

Crosslinking efficiency investigation

The scaffold stability and integrity are essential to accomplish its function when implanted in the human body. To prevent the dissolution of the polymer components in body fluids, a post-processing method, such as crosslinking is required. It should be stated that we assume an interaction between SA and CB in the ink, keeping in mind the fast capacity of SA to form gel with calcium ions.
The efficiency of the two-step crosslinking method applied in this study was investigated by GF analysis. After the initial exposure to GA vapors for the initiation of the protein crosslinking, the second step involved the immersion of the scaffold in the crosslinking bath for the combined crosslinking of polymers. Three crosslinking baths were investigated, and differences among them were noticed, as revealed by the GF results in Fig. 1.C. The highest GF value (93.2%) was obtained when using 5C1G crosslinking bath, determining its choice for subsequent crosslinking experiments.

Shape retention ability

One of the main challenges in 3D printing field is related to the shape retention ability of predesigned scaffold. The consistency of paste-type ink was an important parameter to prevent the strands collapse or filaments merging. The shape fidelity of both uncrosslinked and crosslinked structures to the designed model was highlighted in Fig. 1.A. The micro-CT image illustrated the microstructure of FGCA scaffold, namely the homogeneous distribution of all three components, as depicted in Fig. 1.B.

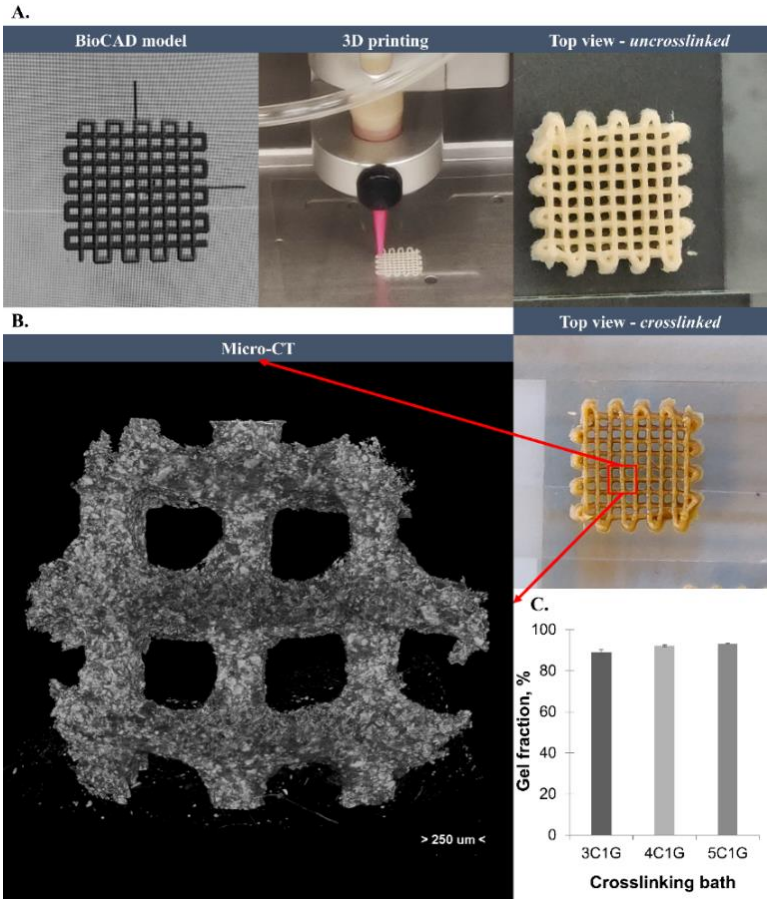

Fig. 1.A. Digital images illustrating the BioCAD model, the scaffold`s printing and the top view of uncrosslinked and crosslinked samples; B. Representative micro-CT image of FGCA scaffold; C. GF results corresponding to the crosslinking study (values reported are an average of n= 4, ± standard deviation)

Structural and dimensional stability

The swelling capacity of hydrogels in aqueous media is an important property that causes notably changes in weight and size. Fig. 2.A illustrated the aspect of dried and rehydrated FGCA structures which maintained their rectangular shape in both states. The swelling results of FGCA scaffold were shown in Fig. 2.B, illustrating that the maximum swelling degree (162.31%) was reached at 28 hours. Dimensional changes were also determined at the equilibrium point and were plotted in Fig. 2.C. The smallest dimensional modification was registered for the height parameter (12.38%), while Δd for width and length were 18.18% and 19.86%, respectively. Therefore, the swelling results and the dimensional changes highlighted the stability of FGCA hybrid scaffold in aqueous media.

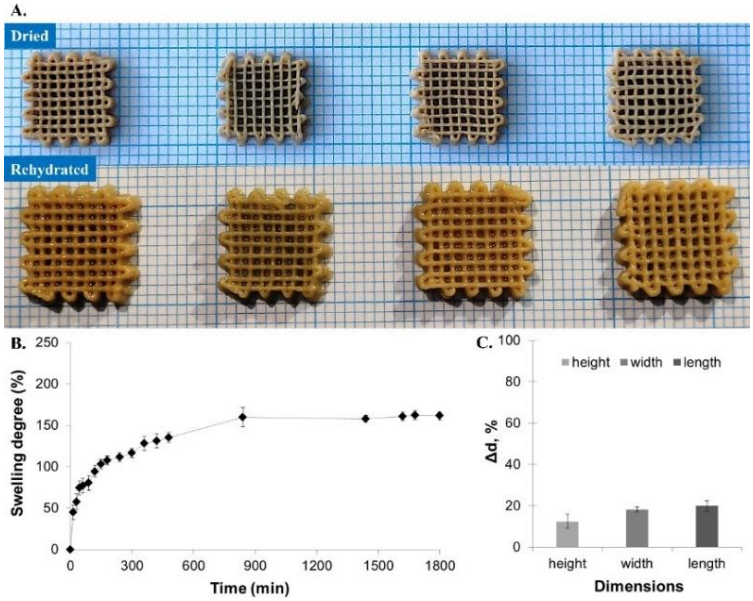

Fig. 2.A. Digital images for dried/ rehydrated FGCA structures; B. Swelling behavior of hybrid scaffold; C. Dimensional modifications of L / W / H at equilibrium point of swelling

Degradation behavior in PBS

The results of the degradation experiment were presented in Fig. 3. After 7 days of incubation in PBS, the printed scaffolds have reached a DD of 6.25 ± 0.39%, while after 28 days, their DD was 37.26 ± 3.80% (Fig. 3.A). Despite these DD values, the stability and integrity of the FGCA scaffolds was not affected, which might indicate the crosslinking efficiency and compatibility between components. Fig. 3.A highlighted the aspect of PBS-degraded samples after 7 and 28 days; the scaffolds preserved their shape fidelity to the predesigned model.

The structural and compositional changes of FGCA scaffolds caused by the degradation in PBS were investigated by FTIR analysis. To this end, spectra of raw materials and FGCA scaffolds before and after 7 and 28 days of incubation in PBS were recorded, as shown in Fig. 3.B, and were compared with each other. The main absorption bands characteristic to the functional groups attributed for each component have facilitated their identification in the printed scaffold. The signals specific to O–H and N–H groups are attributed to both polymeric components and are observed in the wavenumber interval from around 3277 to 3420 cm^{-1}. The specific absorption bands of the protein were visible due to amide I presence around 1635 cm^{-1}, amide II at approximately 1525 cm^{-1}, and N–H bending vibration around 1240 cm^{-1}. The main absorption bands of alginate were represented by the stretching vibration of O-H in the wavelength range of 3000 to 3600 cm^{-1}, by the stretching vibrations at approximately 1405 cm^{-1} which are assigned to C=O bonds from the carboxylate salt groups, by those of C-O

observed around 1335 cm^{-1}, and by those of C-O-C and C-C around 1026 cm^{-1}. The presence of the CB was noticed due to the signals associated with β-chitin and aragonite, the meta-stable form of calcium carbonate. The characteristic absorption bands corresponding to aragonite were represented by the CO_3^{-2} vibrations at approximately 706 and 716 cm^{-1}. The absorption band of C-O around 853 cm^{-1} was also attributed to aragonite, while the absorption bands at approximately 1645 cm^{-1} (Amide I) was attributed to the organic phase of CB, mainly β-chitin. The stretching vibration of C-O observed around 1079 cm^{-1} was also specific to β-chitin. As shown in Fig. 3.B, the spectra of FGCA scaffold before immersion in PBS combined the main absorption bands specific to the both polymers and some of the characteristic bands for CB.

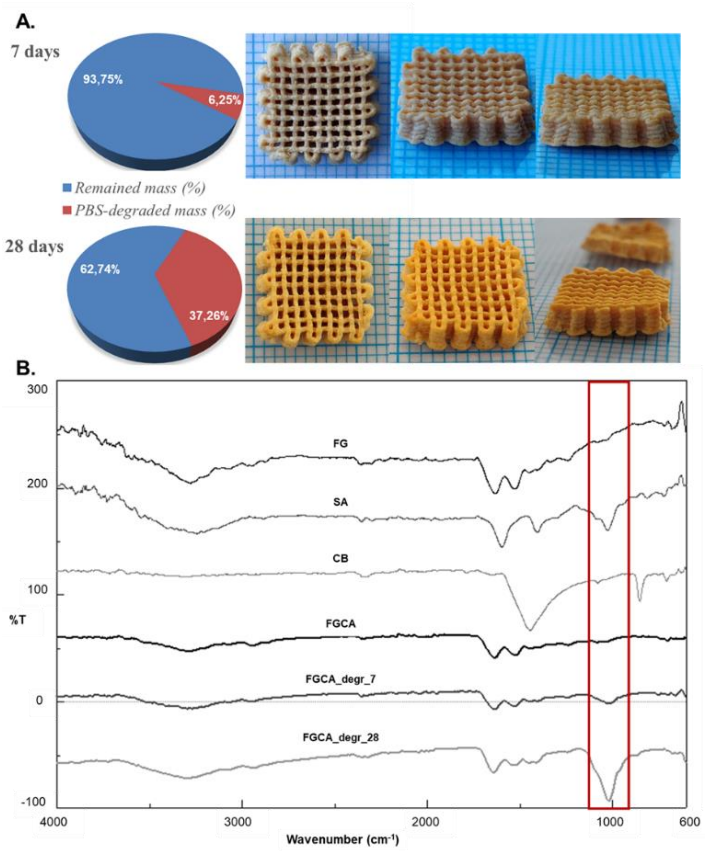

Fig. 3. Degradation assessment: A. Representation of PBS-degraded mass and digital images of a representative sample after 7 days and 28 days of incubation in PBS; B. FTIR spectra corresponding to the raw materials (FG, SA, CB) and to the hybrid scaffolds before degradation (FGCA) and after degradation at 7 days (FGCA_degr_7) and 28 days (FGCA_degr_28)

The spectra of the PBS-degraded scaffolds also presented a combination of vibrations assigned to both polymers and biogenous material. However, some

structural changes in the spectra were observed depending on the incubation period and degradation degree. After 7 days of incubation in PBS, the spectra of FGCA scaffold which presented a low DD was not significantly different in comparison with the scaffold spectra recorded before incubation, while after 28 days of incubation in PBS, the stretching vibrations of C-O-C and C-C corresponding to the alginate component become more visible. This main spectral change was noticed around 1020 cm^{-1} in the spectra of both FGCA_degr_7 scaffold (FGCA scaffold incubated 7 days in PBS) and FGCA_degr_28 scaffold (FGCA scaffold incubated 28 days in PBS). It may be possible that the incubation in PBS determines a matrix reorganization caused by the degradation process and, eventually, a better exposure of the polysaccharide. This will be further investigated, in a different work.

Mechanical behavior

In a previous study of our group, the reinforcing effect of CB dispersed in a hydrogel membrane was highlighted in comparison with other well-known fillers incorporated in the gelatin/alginate membrane [5].

In this work, a concentrated ink was used for the fabrication of FGCA printed scaffolds, as the formulated composition may play an important role to achieve a high stiffness. For instance, the data reported on the mechanical properties of 3D printed scaffolds based on concentrated inks have demonstrated that the Young modulus was significantly superior compared to the data obtained on compositions with lower concentrations [22], [23]. The compressive modulus of concentrated gelatin/alginate/hydroxyapatite scaffolds (in hydrated state) with different mass ratio (39/30/31 or 50/30/20) varied approximatively between 1.25 MPa and 2.2 MPa, as shown in their graphical representation [22].

In our study, the FGCA scaffolds have reached a Young modulus of 1.37 ± 0.15 MPa, in the rehydrated state, with an EC_{PBS} of 61.64%, indicating a high stiffness, as shown in Fig. 4.A. The data stated the influence of concentrated ink and the reinforcing effect of the biogenous material for reaching such promising results. Moreover, the integrity of all tested FGCA scaffolds was maintained during the compression testing, as revealed in Fig. 4.B.

The changes in Young modulus value of scaffolds incubated 28 days in PBS were also investigated. A decrease with 62.8% (from 1.37 MPa of undegraded scaffold to 0.51 MPa of degraded scaffold) of Young modulus value was noticed after a DD of 37%. However, the incubation in PBS does not led just to the scaffold degradation, it also ensured the matrix reorganization and provided much more elasticity to the scaffold. No fragmentation of the scaffold structure was noticed, only a superficial crack, as shown in Fig. 4.C.

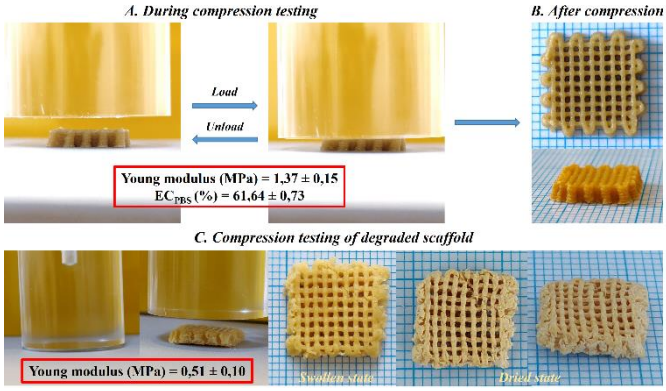

Fig. 4.A. Representative digital images during compression testing (inset revealing the Young modulus achieved and the corresponding EC_{PBS}); B. Digital images revealing the scaffolds integrity after compression test; C. Compression testing of degraded scaffold after 28 days incubation in PBS - representative digital images

4. Conclusions

A concentrated ink based on FG, SA and CB has been formulated to facilitate the printability with high accuracy and to stimulate the shape fidelity. The formulated composition was remarkably involved in reaching such appealing properties for FGCA printed scaffold. A GF value above 93% has confirmed the crosslinking efficiency, predicting the stability of the hybrid scaffold. The swelling results, the dimensional changes, and the degradation experiment have proved the scaffold stability in PBS. The potential of the biogenous bone as a reinforcing filler was highlighted by the promising Young modulus value (1.37 MPa). Therefore, this study sustains the promising features of CB-loaded scaffolds and suggests the FGCA scaffold potential as interesting bone substitute for bone tissue repair.

Acknowledgments

3D printing and Micro-CT analysis were possible due to ERDF / COP 2014-2020, ID P_36_611, MySMIS 107066, INOVABIOMED.

R E F E R E N C E S

[1] *A. S. Neto and J. M. F. Ferreira*, "Synthetic and marine-derived porous scaffolds for bone tissue engineering," Materials (Basel)., vol. 11, no. 9, p. 1702, Sep. 2018.

[2] *J. Cadman, S. Zhou, Y. Chen, W. Li, R. Appleyard, and Q. Li*, "Characterization of cuttlebone for a biomimetic design of cellular structures," Acta Mech. Sin. Xuebao, vol. 26, no. 1, pp. 27–35, Mar. 2010.

[3] *M. R. A. Siddiquee, A. Sultana, and A. Siddique*e, "Scientific Review of Os Sepia (Jhaag-e-Darya / Samudra Phena) with Respect to Indian Medicine and its Characterization on Physicochemical Parameters," vol. 2, no. 26059688, 2014.

[4] *J. Cadman, S. Zhou, Y. Chen, and Q. Li*, "Cuttlebone: Characterisation, Application and

Development of Biomimetic Materials," J. Bionic Eng., vol. 9, no. 3, pp. 367–376, 2012.
[5] *D. M. Dragusin et al*., "Biocomposites based on biogenous mineral for inducing biomimetic mineralization," Mater. Plast., vol. 54, no. 2, pp. 207–213, Jun. 2017.
[6] *X. Zhang and K. S. Vecchio*, "Conversion of natural marine skeletons as scaffolds for bone tissue engineering," Front. Mater. Sci., vol. 7, no. 2, pp. 103–117, 2013.
[7] *J. S. Park, Y. M. Lim, M. H. Youn, H. J. Gwon, and Y. C. Nho*, "Biodegradable polycaprolactone/cuttlebone scaffold composite using salt leaching process," Korean J. Chem. Eng., vol. 29, no. 7, pp. 931–934, Jul. 2012.
[8] *K. Periasamy and G. C. Mohankumar*, "Sea coral-derived cuttlebone reinforced epoxy composites: Characterization and tensile properties evaluation with mathematical models," J. Compos. Mater., vol. 50, no. 6, pp. 807–823, 2016.
[9] *G. Xu, H. Li, X. Ma, X. Jia, J. Dong, and W. Qian*, "A cuttlebone-derived matrix substrate for hydrogen peroxide/glucose detection," Biosens. Bioelectron., vol. 25, no. 2, pp. 362–367, 2009.
[10] *A. Mourak, M. Hajjaji, and A. Alagui*, "Cured cuttlebone/chitosan-heated clay composites: Microstructural characterization and practical performances," J. Build. Eng., vol. 26, no. May, p. 100872, 2019.
[11] *L. O. Vajrabhaya, S. Korsuwannawong, and R. Surarit*, "Cytotoxic and the proliferative effect of cuttlefish bone on MC3T3-E1 osteoblast cell line," Eur. J. Dent., vol. 11, no. 4, pp. 503–507, Oct. 2017.
[12] *A. Rogina, M. Antunović, and D. Milovac*, "Biomimetic design of bone substitutes based on cuttlefish bone-derived hydroxyapatite and biodegradable polymers," J. Biomed. Mater. Res. - Part B Appl. Biomater., vol. 107, no. 1, pp. 197–204, 2019.
[13] *A. S. Neto, D. Brazete, and J. M. F. Ferreira*, "Cuttlefish bone-derived biphasic calcium phosphate scaffolds coated with sol-gel derived bioactive glass," Materials (Basel)., vol. 12, no. 7, p. 2711, Aug. 2019.
[14] *S. Poompradub, Y. Ikeda, Y. Kokubo, and T. Shiono*, "Cuttlebone as reinforcing filler for natural rubber," Eur. Polym. J., vol. 44, no. 12, pp. 4157–4164, Dec. 2008.
[15] *S. Shang, K. L. Chiu, M. C. W. Yuen, and S. Jiang*, "The potential of cuttlebone as reinforced filler of polyurethane," Compos. Sci. Technol., vol. 93, pp. 17–22, 2014.
[16] *S. García-Enriquez et al*., "Mechanical performance and in vivo tests of an acrylic bone cement filled with bioactive Sepia officinalis cuttlebone," J. Biomater. Sci. Polym. Ed., vol. 21, no. 1, pp. 113–125, 2010.
[17] *Z. Okumuş and Öm. S. Yildirim*, "The cuttlefish backbone: A new bone xenograft material?", Turkish J. Vet. Anim. Sci., vol. 29, no. 5, pp. 1177–1184, 2005.
[18] *E. Dogan and Z. Okumus*, "Cuttlebone used as a bone xenograft in bone healing," Vet. Med. (Praha)., vol. 59, no. 5, pp. 254–260, 2014.
[19] *D. Chawla, T. Kaur, A. Joshi, and N. Singh*, "3D bioprinted alginate-gelatin based scaffolds for soft tissue engineering," Int. J. Biol. Macromol., vol. 144, pp. 560–567, 2020.
[20] *Y. Zhang et al*., "Biomaterials based on marine resources for 3D bioprinting applications," Marine Drugs, vol. 17, no. 10. 2019.
[21] *A. Serafim, S. Cecoltan, A. Lungu, E. Vasile, H. Iovu, and I. C. Stancu*, "Electrospun fish gelatin fibrous scaffolds with improved bio-interactions due to carboxylated nanodiamond loading," RSC Adv., vol. 5, no. 116, pp. 95467–95477, 2015.
[22] *Y. Luo, A. Lode, A. R. Akkineni, and M. Gelinsky*, "Concentrated gelatin/alginate composites for fabrication of predesigned scaffolds with a favorable cell response by 3D plotting," RSC Adv., vol. 5, no. 54, pp. 43480–43488, 2015.
[23] *Y. Luo, Y. Li, X. Qin, and Q. Wa*, "3D printing of concentrated alginate/gelatin scaffolds with homogeneous nano apatite coating for bone tissue engineering," Mater. Des., vol. 146, pp. 12–19, 2018.